MAVACS - a new system creating a non-magnetic environment for palaeomagnetic studies

K. PŘÍHODA; M. KRS; B. PEŠINA AND J. BLÁHA
Geofyzika N. C., Brno, Prague Division, Geologická 2, 152 00 Prague 5 Barrandov (Czechoslovakia)

ABSTRACT

An automatic feedback system of three units called MAVACS (Magnetic Vacuum Control System) providing triaxial compensation of the Earth's magnetic field and its variations which yields max. ± 2 nT deviation from zero in 5 l volume is described. A large size Helmholtz induction coil unit HELICOS supplied by induction coil control unit ICCON produces triaxial compensating magnetic field. Deviation of the fields is measured by rotating coil magnetometer ROCOMA which controls ICCON to suppress the deviation to zero. Unique magnetometer design using non-magnetic sensor with rotating coil being borne and high speed driven by compressed air yields ± 0.1 nT typical offset from zero and low noise. Unit operating principles, block diagrams, magnetometer sensor construction and methods of its signal processing are presented as well.

The paper also presents case histories indicating magnetic purity in the analysis of the remanent magnetization structure of genetically different rocks by means of the MAVACS system. Examples of practical use are given for palaeovolcanics, sediments with detritic magnetization, sediments with chemoremanent magnetization, strongly remagnetized rocks of the red beds type and organogenic limestones. Some of these rocks were affected by a number of phases of orogenic activity. The high magnetic vacuum, created by the MAVACS proved to be necessary for the quantitative analysis of multi-component magnetization.

INTRODUCTION

Palaeomagnetic data derived from rocks of different geneses in various world laboratories have yielded a lot of information on global tec-

tonics and other geological disciplines. Problems, some of which are due to laboratory techniques, have arisen, however, in the interpretation of palaeomagnetic data. Especially the introduction of the multi-component analysis of magnetization makes it necessary for the individual magnetization components to be determined with high accuracy. This technique requires progressive demagnetization to be performed in a highly non-magnetic environment.

In palaeomagnetic studies of rocks strongly affected by orogenic processes, or of rocks remagnetized in the geological past, it may be difficult to reproduce the palaeomagnetic components. Such rocks require progressive demagnetization, generally in a thermal regime, as a rule up to the Curie temperature of magnetite or haematite. In the course of thermal demagnetization, minerals with magnetically soft properties often appear in the samples so that demagnetization has to be carried out in a non-magnetic environment. Numerous experiments carried out on pre-Variscan rocks of the Barrandian (Bohemian Massif) have shown that in a non-magnetic furnace even a residual magnetic field of an intensity of a few tens of nanotesla can be a source of undersirable sample magnetization.

The above mentioned factors formed the basis for the development of a system which creates a magnetic vacuum in a space of about 5 litres below a value of $\pm$ 2 nT, the typical offset of the magnetic field sensor being smaller than $\pm$ 0.1 nT. The system was experimentally tested by systematic measurements conducted for a time period of over three years, and given the name MAVACS, Magnetic Vacuum Control System. Multi-component analysis of the structure of the remanent magnetization and reproduction of the palaeomagnetic directions even in rocks whose magnitude of secondary magnetization represents 97 to 99 % of the magnitude of natural remanent magnetization, can be achieved accurately with this system.

The first part of the present work deals with the design of the MAVACS apparatus describing the block diagrams of the system function moduli and the method of signal processing. A detailed description is given of the principles of the function and mechanical construction of the unique magnetic field sensor with a rotating coil placed in a rotor, which is borne and high-speed driven by compressed air. The second part of the work presents case histories indicating magnetic purity in the analysis of the remanent magnetization structure of genetically different rocks by means of the MAVACS.

OPERATING PRINCIPLE

The Magnetic Vacuum Control System MAVACS is a self-contained automatic system creating a limited space with the magnetic field elimi-

nated i.e. a non-magnetic environment or magnetic vacuum. Field elimination is achieved by means of a compensating method using an artificial magnetic field to compensate the natural magnetic field of the Earth. The Earth's magnetic field vector is a time variable physical quantity, changing both its magnitude and direction. Consequently, the artificial field vector is to be controlled in magnitude and direction to ensure precise variation-free compensation. It is achieved by composing the compensating vector from three individually controllable rectangular field components fixed in space.

THREE UNITS FORMING MAVACS

The MAVACS system is composed of three units forming a feedback loop continuously compensating the Earth's magnetic field, ref. Fig. 1.

The three time-varying components of the Earth's magnetic field are compensated by the artificial field of the same direction and magnitude but of opposite polarity produced by electrical currents flowing through a large three component Helmhlotz Induction Coil System HELICOS. Precision of field compensation is continuously monitored by a three channel Rotating Coil Magnetometer ROCOMA, which has its sensors fixed inside the HELICOS. Deviation of any field component from precise compensation causes the ROCOMA magnetometer to produce an eletrical control signal for a three channel Induction Coil Control Unit ICCON.

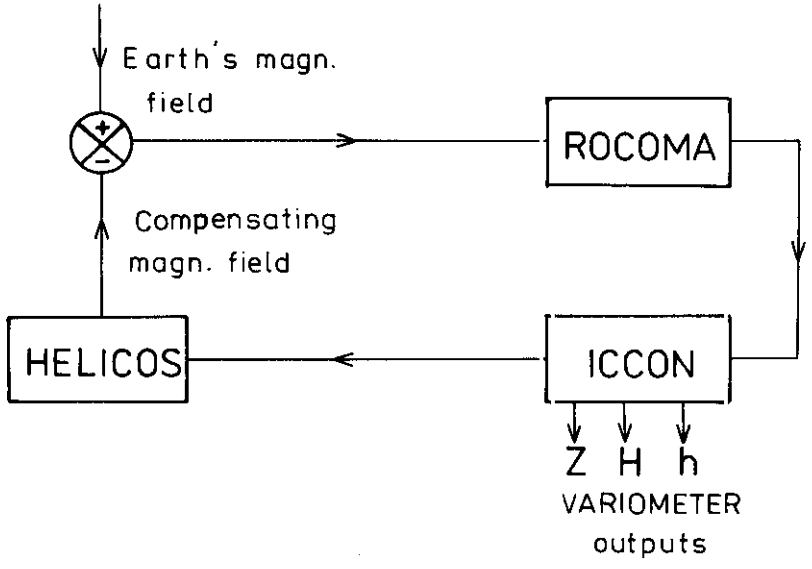

Fig. 1. Block schematic diagram of the MAVACS system.

The ICCON supplies and controls the electrical currents flowing through the HELICOS to eliminate the field deviation. In this way the negative feedback loop of the MAVACS system is completed, creating a high quality non-magnetic environment in the HELICOS centre.

Rocoma

The Rotating Coil Magnetometer ROCOMA is the heart of the MAVACS system, being an instrument designed for three component measurements of the magnetic field vector within the range of 0.1 nT to 100.000 nT. The main feature of the ROCOMA is its non-magnetic sensor using a rotating coil which is both borne and high speed driven by compressed air. The classic rotating coil principle, well proven in the early «Earth's inductor», secures magnetometer zero to an accuracy of ± 0.1 nT, while making use of the present state-of-the-art in mechanical and electronic engineering yields 0.02 nT peak to peak typical magnetometer noise in a 0 to 0.1 Hz bandwidth.

The ROCOMA can be applied in four basic modes of operation. It can operate either as a self-contained absolute or differential magnetometer, or as a fundamental part of the MAVACS system securing variation-free creation of either the non-magnetic environment with a typical offset from zero less than ± 0.3 nT, or three component calibration fields within the range of 0 to ± 10.000 nT. The ROCOMA magnetometer cosists of:

— two sensors, each having a coil inside a rotor rotating on 20.000 rev/min and a device for rotor position measurement

— one electronic unit which filters noise, resolves the sensor signal into two rectangular components and controls sensor rotor position & speed

— one air unit which processes the air supply delivered to the sensors for rotor bearings and driving jets

— one air compressor which provides compressed air to supply the sensors.

The basic parts of the ROCOMA magnetometer are described in the following sections.

Sensor

The sensor converts the magnetic field into alternating signal voltage. Its most important parts are the rotating coil and an optical device for coil position measurement. The coil generates a sine-wave signal with an amplitude proportional to the magnetic field vector magnitude, while the

phase shift of the signal yields information about the vector direction. The measured magnetic field vector $\bar{B}$ is resolved to its components in the cartesian coordinates x, y, z defined inside the sensor by the a_r and a_p axes - ref. Fig. 2.

The a_r is the mehanical axis of rotation of the coil (c), while the a_p is optical axis connecting stationary bulb (b) and phototransistor (t).

The a_r and a_p axes are mutually perpendiular and define the ς plain. The a_z axis is perpendicular to the ς plain and intersects with the a_p and a_r axes in the junction point 0 in the coil centre. Along the a_p, a_r, a_z axes are introduced the x, y, z cartesian coordinates having origin 0 and the arrows pointing in the positive directions of the coordinates system. Any magnetic field vector may be resolved into its components $\bar{B}_x$, $\bar{B}_y$, $\bar{B}_z$ (projected on the cartesian coordinate axes) by using the direction cosines of the angles between the vector and the respective coordinate (not depicted in Fig. 2).

Alternating signal voltage $\bar{e}$ generated by the coil rotating in the measured magnetic field is proportional to the rate of change of the flux $\bar{\phi}$ existing inside the coil area and to the number n of the coil turns

$$\bar{e} = - n \frac{d\bar{\phi}}{dt} \tag{1}$$

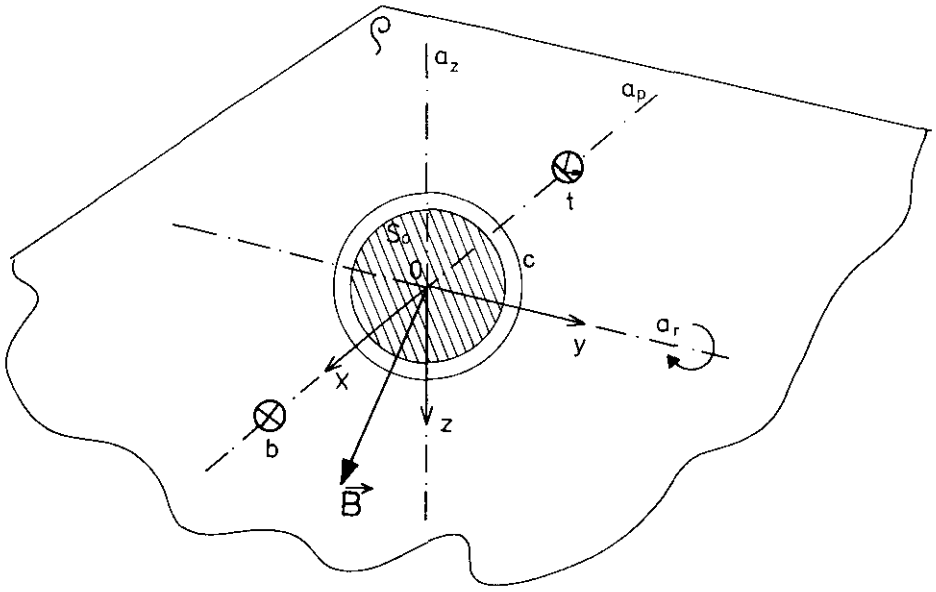

Fig. 2. Cartesian coordinates x, y, z of the ROCOMA sensor. Rotating coil (c) is depicted in the fundamental coil position in which the a_p axis coincides with the coil mechanical axis.

Let us assume the magnetic field vector $\bar{B}$ is projected on the x coordinate as the $\bar{B}_x$ component and the coil rotates around its a_r axis - ref. Fig. 2(B_x not depicted). The coil flux vector $\bar{\phi}$, is determined by a product of the $\bar{B}_x$ and periodically variable instant coil area S being a projection of the S_o

$\bar{\phi} = \bar{B}_x S$

$S = S_o \cos \varphi = S_o \cos \omega t$

where S_o = nominal coil area (area of circular slanted lining in Fig. 2)
φ = oriented angle between the $\bar{B}_x$ component (x coordinate) and the rotating mechanical axis of the coil winding (in the fundamental coil position of Fig. 2 this rotating winding axis coincides with the a_p axis and $\varphi = 0$; the winding axis and φ not depicted in Fig. 2)
ω = angular speed of the coil rotation
t = time

From the above it follows

$$\bar{e}_x = - n \frac{d\bar{\phi}_x}{dt} = - n \bar{B}_x \frac{dS}{dt} = n \bar{B}_x S_o \omega \sin \omega t \qquad (2)$$

Similarly, the $\bar{B}_z$ component of the $\bar{B}$ vector originates the $\bar{e}_z$ signal component being 90° shifted in respect to the $\bar{e}_x$

$$\bar{e}_z = n \bar{B}_z S_o \omega \cos \omega t \qquad (3)$$

The signal voltage $\bar{e}$ generated by the ROCOMA sensor is proportional to the magnetic field vector magnitude, nominal coil area, its number of turns and the angular speed of coil rotation. If using the real sensor parameters, the Eq. 2, 3 give 5 microvolt peak signal amplitude on 1 nT field.

The signal voltage $\bar{e}$ can be considered as being composed of two rectangular (90° shifted) signal components $\bar{e}_x$, $\bar{e}_z$ corresponding to the two rectangular components $\bar{B}_x$, $\bar{B}_z$ of the magnetic field vector $\bar{B}$. Component resolution is performed by the synchronous detectors in the electronic unit.

$\bar{B}_y$ component of the $\bar{B}$ vector generates zero flux $\bar{\phi}$ due to the fact the nominal coil area S_o projected into the y coordinate direction gives zero instant area S. Thus $\bar{e}_y = 0$. The ROCOMA sensor is insensitive to a magnetic field component coinciding with the a_r axis of the coil rotation. Consequently, two sensors are needed to perform simultaneous three component measurements of the magnetic field vector.

The operating principles outlined in Fig. 2 are implemented in a compact sensor having its coil mounted inside a rotor both borne and driven by compressed air. Fig. 3 and Fig. 4 depict sensor parts and accessories fundamental for its practical use.

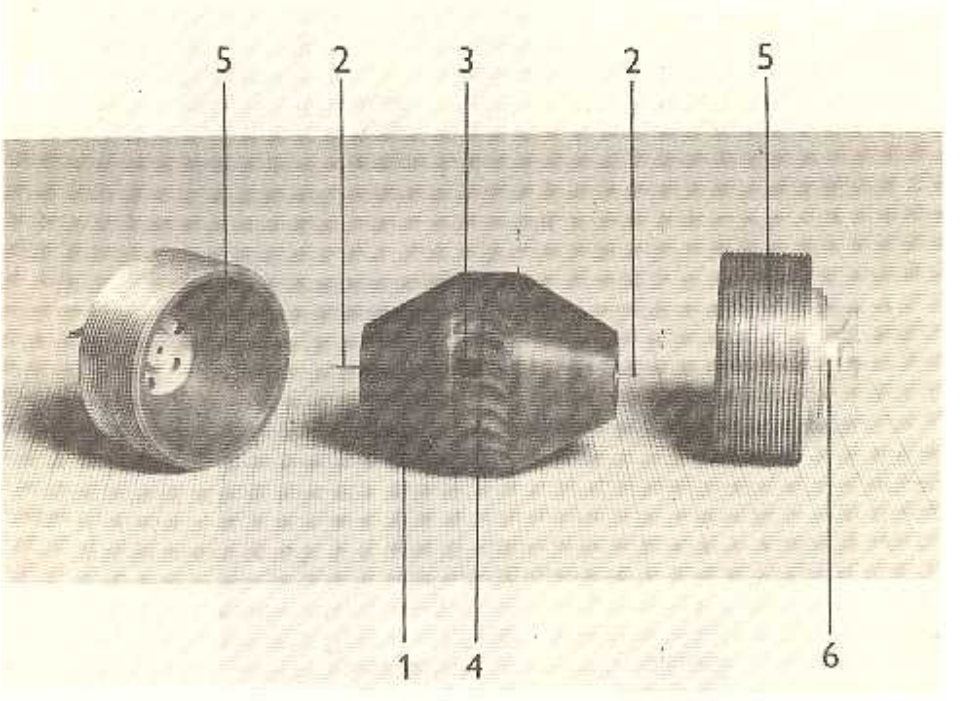

Fig. 3. Sensor rotor and its main accessories.
1. sensor rotor (built — in coil with 8000 turns and 20.5 mm diameter is invisible)
2. coil contact pin (platinum)
3. light channel (its axis coincides with the mechanical axis of the coil winding. The rotating light channel is part of the coil position measuring device generating a sequence of pulses in its phototransistor. Each pulse occurs precisely at the instant when the coil is in its fundamental position, depicted in Fig. 2)
4. driving blade
5. air bearings (there are eight barely visible air jets on the conical surface)
6. contact cell (there is a drop of mercury inside the cell connecting the coil contact pin with the cell stationary lead)

Electronic unit

The electronic unit contains most of the ROCOMA electronic circuits. In general it facilities magnetometer settings to any of its four operatio-

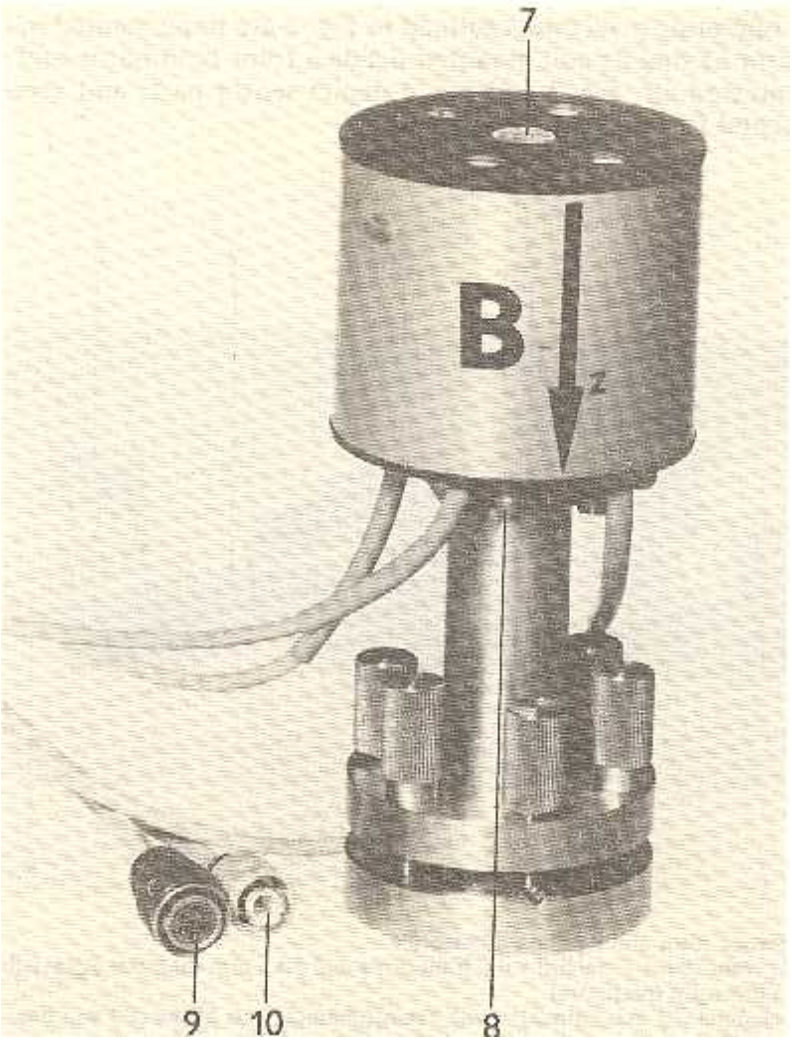

Fig. 4. Complete ROCOMA sensor.

7. level gauge (facilitates horizontal adjustment of the ρ plain typical for most sensor applications)
8. one of the two sensor air inlets (bearing, driving air)
9. connector and 10 m long shielded cable (links the non-magnetic sensor bulb with its heating voltage and the phototransistor with the amplifier in the electronic unit — ref. Fig. 5)
10. coaxial connector and 10 m long shielded cable (provides connection of the sensor signal voltage to the A.C. preamplifier in the electronic unit — ref. Fig. 5)

B. the latter distinguishes between the two ROCOMA sensors (A, B) to facilitate standard sensor connections to the ROCOMA units and its standard positioning in the MAVACS system

Z, H. (top) — the arrows designate direction and positive polarity of the two rectangular sensitivity components of the sensor.

nal modes and realizes both the electronic support for the sensor and the sensor signal processing. A comprehensive information about electronic unit operation is given in the ROCOMA block schematic diagram (see Fig. 5) and in the brief description which follows.

Sensor electronic support

The support concerns bulb heating and rotor speed stabilization, which take place in the bulb control and the speed control blocks. The blocks are controlled by the train of phototransistor pulses being generated in the coil position measuring device of the sensor and amplified in the amplifier block.

In the bulb control block there is a source heating the bulb by a 20 kHz alternating voltage to secure easy elimination of the disturbing signals due to high-intensity heating currents flowing near the sensor coil. Moreover, the bulb heating voltage is automatically controlled to stabilize amplitude of the phototransistor pulses, which is a precondition for securing high accuracy of the coil position measuring device. If the bulb

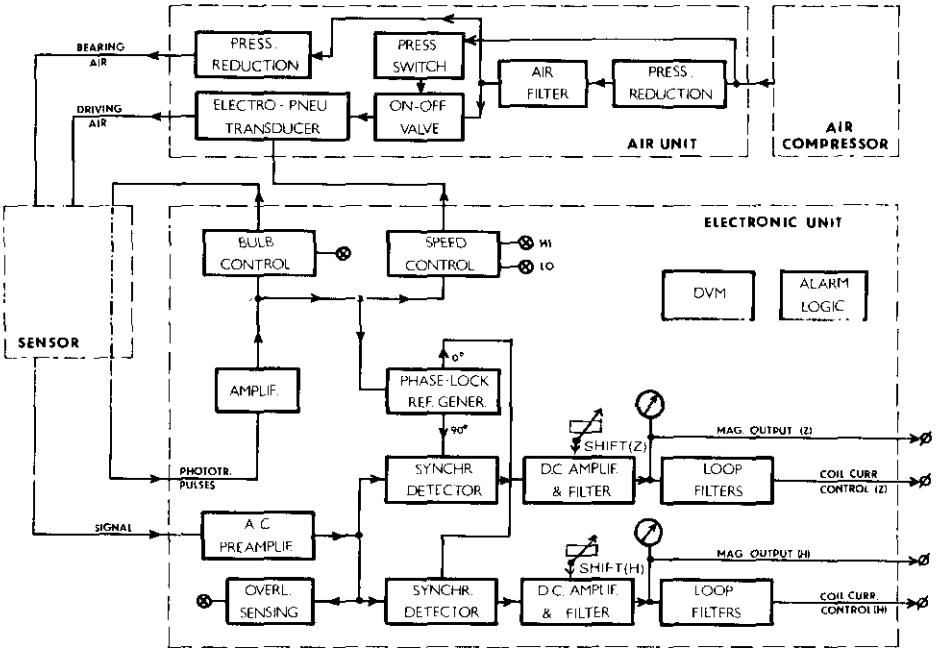

Fig. 5. ROCOMA block schematic diagram depicting two channels.

heating voltage approaches the maximum specified, a front panel «Weak bulb» signal lamp is gradually switched on.

The speed control block measures frequency of the train of the phototransistor pulses (approx. 330 Hz) and generates control voltage for the electro-pneu transducer of the air unit which supplies air to the rotor driving jets. In this way the rotor speed is stabilized, this being a precondition for stabilizing magnetometer sensitivity. Sensor speed deviation exceeding the limit of approx. ± 0.2 % is indicated on the ROCOMA front panel by signal lamps «High speed», «Low speed» and the sound alarm is activated in the alarm logic block. If ROCOMA operates in the MAVACS system the alarm logic block also automatically discontinues the MAVACS loop.

Signal processing

The most important tasks of the ROCOMA signal processing system are the resolution of the magnetic field vector into two rectangular components and very efficient signal filtering so as to achieve suppression of magnetic field disturbances and noise. Among the other important tasks are high-accuracy signal voltage amplification, ROCOMA frequency response correction (needed to make the MAVACS loop stable) and prompt magnetometer settings to any of its four operational modes. The methods used to fulfil the above specified tasks are described in the following sections referring also to the block schematic diagram.

The A. C. preamplifier block provides high input impedance for the sensor signal voltage and low-noise wideband amplification. The preamplifier alternating output signal is apllied to the pair of the synchronous detector blocks and the overload sensing block. The overload sensing block indicates signal excursions exceeding the specified maximum by both the «Over load» signal light and the sound alarm activated in the alarm logic block. If the ROCOMA is set to its MAVACS system operational mode, the alarm logic block also automatically discontinues the MAVACS loop.

The ROCOMA signal processing system utilizes the crosscorrelation method of signal detection. This method is based on multiplication of the detected signal by a so-called coherent reference signal which has a zero or constant phase shift with respect to the sensor signal. The multiplication of the coherent alternating signals results in a D. C. signal proportional to the sensor signal magnitude and cosine of its phase shift with respect to the coherent reference. Non-coherent signal multiplication yields exclusively alternating output.

The coherent reference signal is generated in the phase-lock reference generator. This is an integral part of the coil position measuring device

and the ROCOMA signal processing system. It generates two square-wave signals, one being exactly in-phase (zero phase shift), the other exactly out-of phase (90° shift) relative to the train of phototransistor pulses. These two reference square-wave signals are thus coherent with the two sensor signal comonents $\bar{e}_x$, $\bar{e}_z$ corresponding to the two rectangular components $\bar{B}_x$, $\bar{B}_z$ of the magnetic field vector $\bar{B}$.

The crosscorrelation method of signal detection is realized in the pair of the synchronous detector blocks performing essentially the signal multiplication. Crosscorrelation of the $\bar{e}_x$, $\bar{e}_z$ sensor signal components (comprised in the detected signal) with the in-phase and the out-of phase reference signals yields useful detector D. C. output signals representing resolved components proportional to the rectangular field components $\bar{B}_x$, $\bar{B}_z$ respectively. Crosscorrelation of non-coherent disturbances and noise dominating in the detected signal results in alternating detector output being suppressed in the following blocks.

The D. C. amplifier & filter block provides various functions associated with both the signal processing and the ROCOMA settings to its operational modes. There are two basic ROCOMA settings in this block, making the particular ROCOMA channel (Z or H in Fig. 5) operate either as a self-contained magnetometer or as part of the MAVACS system.

In the magnetometer mode of ROCOMA measurement the block operates as a step-controlled D. C. amplifier securing the three basic magnetometer ranges (± 1 nT, ± 10 nT, ± 100 nT) along with the noise suppression due to filtering time constants (max. 8 s response time on ± 1 nT range).

If using ROCOMA in both the MAVACS system operational modes, the amplifier operates as a signal integrator to implement ROCOMA frequency response correction, securing MAVACS system feedback loop stability and very accurate compensation of slow Earth's magnetic field variations. The settings facilitated in the block enable the channel to operate either in the magnetic vacuum control mode or in the magnetic field generation mode of the MAVACS system. Because of the fact that the non-magnetic environment is only a specific magnetic field— zero field— the ROCOMA operations differ only slightly. The bipolar D. C. shift signal is applied in both the modes as the ROCOMA sensors operate off the HELICOS centre to keep the valuable non-magnetic environment free for the applications. To achieve a non-magnetic environment in the HELICOS centre, a specific low-level magnetic field must be adjusted in the sensor sites. This is done by adjusting the shift signals.

The output signal of the D. C. amplifier & filter block is brought either to the front panel deflection meters, to the digital voltmeter in the DVM block and to the output terminals if using ROCOMA in its magnetometer measurement mode, or to the loop filters if using it in the MAVACS system. In either mode the output signal levels are monitored and

if they exceed the preset levels the sound alarm is activated in the alarm logic block and the MAVACS loop is discontinued.

The loop filters suppress high-frequency products of synchronous signal detection to prevent interference in the MAVACS loop. The outputs of the loop filters are used to control the D. C. currents generated by the ICCON which supplies the HELICOS.

Air unit

The air unit processes the air supply delivered to the sensors from the external compressor. In the pressure reduction block the unit reduces first the compressor source air to the stabilized operating air pressure and after being filtered in the air filter block it splits in the bearing air and the driving air paths.

In the bearing air path there is a pressure reduction block facilitating manual set of the constant air pressure for the sensor bearings.

In the driving air path there are the on-off valve and the electro-pneu transducer, which is electrically controlled to keep the sensor rotor revolutions stable. The on-off valve is electrically controlled by the pressure switch which guards the source air pressure of the compressor. If this is not suffcient, the driving air path is automatically discontinued to bring the sensor rotor to a standstill before its bearings lose performance.

Air compressor

The air unit processes the air suplly delivered to the sensors from the ce of the compressed air delivering approx. 50 normal litres/min. It operates as a self-contained device requiring little attention.

ICCON

The Induction Coil Control Unit ICCON is a three channel source of controllable direct electrical current. It has been designed to supply and control current in triaxial Helmholtz induction coils compensating the Earth's magnetic field. The design was tailored to meet the specific needs of rock-sample demagnetization in palaeomagnetic and petrophysical studies.

Control of the current in each of the three ICCON channels is individual and it is achieved by means of the Current control system and the Digital programmer - ref. Fig. 6.

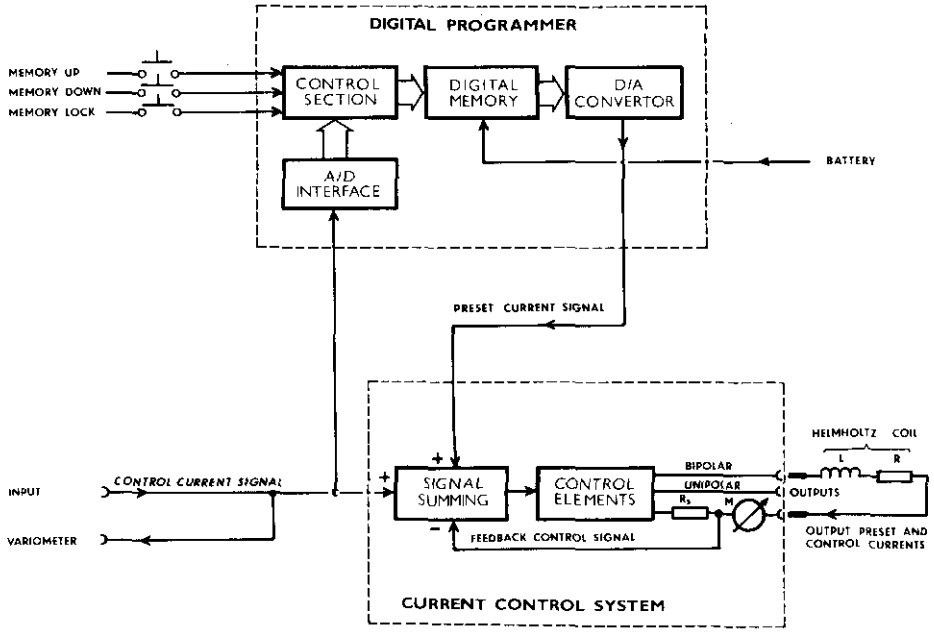

Fig. 6. ICCON block schematic diagram depicting one channel.

The Current control system is an analog negative feedback device converting the control and preset current signals into the control and preset output currents flowing through the Helmholtz coils. The feedback system secures both the accuracy of the conversion and high-speed response of the control output current to the control current signal.

The signal summing block carries out addition and subtraction of its input voltage signals and generates signal algebraic sum on its output. In this way the added preset and control current signals are compared with the subtracted feedback control signal, which represents the preset and control output currents. Any deviation makes the sum non-zero and controls the control elements to make the signals equal within a 0 to 1 kHz frequency range which is fundamental for MAVACS loop speed and stability.

The Helmholtz coils are connected to one of the outputs depending on whether the generated magnetic field must be unipolar or bipolar. The L and R parameters represent Helmholtz coil inductance and resistance. The R_S is a sampling resistor converting the output currents into feedback control signal voltage. M is a deflection meter indicating the output currents level. The maximum output currents are 1 A unipolar and $\pm$ 0.1 A bipolar.

The Digital programmer is basically a very high stability source of the preset current signal. The required signal level is adjustable either ma-

nually or automatically by means of the control section. Manual adjustment is carried out by means of the up or down buttons, which activate a device increasing or decreasing the preset current signal by means of bipolar increments. Automatic signal level adjustment is carried out in the control section by means of the A/D interface being controlled by the analog control current signal. If this signal exceeds a particular level the A/D interface is activated and the control section then incrementally increses or dereases the preset current signal, thus actually bringing about a bidirectional transfer of control output current portions into preset output current.

The control section determines the address to the digital memory which generates the preset current signal in digital form, being converted to analog in the digital to analog convertor. The digital memory is continuous (non-volatile) due to internal battery.

The manual and automatic adjustment of the preset current signal can be inhibited by means of the lock button which is needed if recording the Earth's magnetic field variations on the variometer terminals.

The ICCON can be applied in the stabilization or automatic current control mode of operation depending on the required quality of the non-magnetic environment.

The stabilization mode is suitable for less demanding applications which can tolerate variations of the Earth's magnetic field. In this mode the ICCON operates as a self-contained instrument generating output current of preset value (stable to ± 200 ppm.) being adjusted manually by the up or down buttons incrementing or decrementing the digital memory output. If the ICCON mains supplies are turned off the digital equivalent of the preset output current will be retained in the continuous digital memory, securing precise output current reproduction when resuming ICCON operation.

In its automatic control mode the ICCON operates in the MAVACS loop and generates both the preset and the control output currents to facilitate the creation of a variation —free non— magnetic environment. The preset output current compensates the dominating Earth's magnetic field mean value (typically tens thousands of nT) while the control output current compensates the field variations.

To support continuity of the generated magnetic field i.e. continuity of the magnetic vacuum even during power failures or cuts, the control section continually samples the control current signal by means of the A/D interface. If the signal level exceeds a dead zone equivalent to ± 5 nT the control section increments or decrements the digital memory to transfer the control output current portions equivalent to ± nT into equal preset output current. The preset output current portions can thus be retained during power cuts when the MAVACS loop (i.e. the control current signal) is discontinued. This performance is meaningful if the IC-

CON supplies remain perfect during power cuts. It can be realized by external low-power mains back-up supplies used for the ICCON only.

HELICOS

The Helmholtz Induction Coil System HELICOS is a classic three component device using three pairs of square field coils to produce homogeneous magnetic field in the working space in the centre of the system. The individual coil pairs are spaced to fulfil the familiar Helmholtz condition that the second-order derivative of the field produced along the axis of the coil pairs is zero at the pair centre. This appropiate spacing of the square field coils is 0.5445 of the side of the square.

Accurate calculations of magnetic fields produced in the relatively large working space of the HELICOS were perfomed by application of the well-known Biot-Savart's law combined with numeric integration. This proved to be an effective method for calculating both the coil size necessary to create a working space of the given volume and the field magnitude at any point inside, or even outside the HELICOS system.

From Biot-Savart's law it is obvious the total magnetic field vector $\bar{B}_p$ generated in point P (x, y, z) can be expressed as a product of a vector $\bar{J}$ (J_x, J_y, J_z) representing the electrical currents flowing in the coil conductors, and some transformation representing position of the P point in respect to the conductor system

$$\bar{B}_p = K_p \bar{J}$$

where K_p is a linear transformation which can be expressed as a 3×3 type matrix. If inverting the K_p matrix, the magnitudes of the coil currents corresponding to the requested $\bar{B}_p$ vector magnitude can be calculated

$$\bar{J} = K_p^{-1} \bar{B}_p$$

The actual algorithm for determining the matrix elements is simple in principle but too extensive to be given here.

Using this field representation, both the current vector $\bar{J}_e$ carrying out Earth's magnetic field compensation in the HELICOS centre, and the residual field $\bar{B}_T$ in any linner or outer point of the HELICOS system can be evaluated. Let us denote the linear transformation valid for the HELICOS centre as K_0 and the homogeneous Earth's magn. field, the subject of compensation, as $\bar{B}_e$. The vector of the coil currents $\bar{J}_e$ can then be formally expressed by

$$\bar{J}_e = -K_0^{-1} \bar{B}_e$$

The residual magnetic field $\bar{B}_T$ existing in the P point of the HELICOS system is a superposition of the two fields

$$\bar{B}_T = \bar{B}_e + \bar{B}_p = \bar{B}_e + K_p \bar{J}_e = (K_p - K_o)\, \bar{J}_e$$

The $\bar{B}_T$ can also be expressed as a function of the Earth's mgn. field $\bar{B}_e$ being compensated

$$\bar{B}_T = (K_p - K_o)\, \bar{J}_e = (K_p - K_o).\, (-K_o^{-1})\, \bar{B}_e = (I - K_p\, K_o^{-1})\, \bar{B}_e$$

where I is an identity matrix.

The formal mathematical expressions given in the previous yield practical guidance for the system design. From the last equation it is clear the residual magnetic field $\bar{B}_T$ at any point of the HELICOS system depend also on the Earth's magnetic field magnitude, regardless of the fact that there is a non-magnetic environment (zero field) in the HELICOS centre. This is an important factor which concerns the positioning of the ROCOMA sensors inside the HELICOS system. The sensors must operate outside the valuable working space with non-magnetic environmet and the residual magnetic field $\bar{B}_T$ existing in their actual sites is stabilized as a fixed value by means of the Shift potentiometers of the ROCOMA magnetometer. Variation of the $\bar{B}_T$ vector transforms into equal variation (offset) of the non-magnetic environment in the HELICOS centre. To suppress this effect, the K_p and K_o transformations must be as close to each other as possible. This implies that the sensors be positioned nearest to the HELICOS centre. Computer analysis of the HELICOS system with the actual sensor positions confirmed the result of Earth's magnetic field variations (with amplitudes of max. $\pm$ 100 nT) in the magnetic vacuum not exceeding $\pm$ 0.1 nT.

The outlined mathematical analysis also supported computer-aided design of the HELICOS system, giving quantitative information concerning minimum coil size for the required working space volume (i.e non-magnetic environment volume), necessary coil stability, adjustment accuracy etc. As a result, the HELICOS system yielding a working space volume of approx. 5 litres with max. $\pm$ 2 nT homogeneity deviation was realized by using the square-shaped coils of 2 – 2.5 m size. The coils are attached to the glass frame construction securing stability of the system geometry independent of the environmental parameters and time.

4. EXAMPLES OF THE PRACTICAL USE OF THE MAVACS IN STUDIES OF THE REMANENT MAGNETIZATION STRUCTURE OF GENETICALLY DIFFERENT ROCKS

In the following part, some representative examples are given for rocks in which the respective components of remanent magnetization had to be determined with high accuracy, or which developed phase changes of minerals — the carriers of remanent magnetization — in the course of thermal treatment. The MAVACS was tested by systematic measurements running for over three years, and the results of detailed studies are presented in the works (Krs *et al.*, 1986, 1987; Pruner, 1987). Remanent magnetization was measured on a spinner magnetometer JR-4 (Jelínek, 1966), or on an astatic magnetometer including the magnetic susceptibility in the Earth's magnetic field (Pešina, 1968), the magnetic susceptibility having been measured by a kappa-bridge KLY-2 (Jelínek, 1973). Magnetic susceptibility was measured during the thermal demagnetization of samples so that the posible phase changes of magnetically active minerals could be recognized. Primary data processing was carried out with the use of the program and computer by Šanda (1987), the quantitative multi-component analysis was made by the programs of Chvojka (1987). In order to determine the individual magnetic components forming the natural remanent magnetization and to define the corresponding vectors, algorithms were applied which were based on principal component analysis (Kirschvink, 1980; Schmidt, 1982; Kent *et al.*, 1983). As a rule, the most consistent results were obtained with the use of algorithm LINEFIND (Kent *et. al.*, 1983). The respective components were analyzed statistically in relation to the fold tests, within a layer, a locality and the appurtenant region. The results obtained were collated with the geological and petrographical findings of geologists predominantly from the Geological Survey in Prague.

Experimental work with the MAVACS also indicated the origin of gyromagnetization in the course of measurements on the spinner magnetometer, which led to devising a methodology for measurement with the undesirable prasitic magnetization being suppressed or even eliminated. The rock samples that were termally demagnatized were transported in a non-magnetic environment and measured on the spinner magnetometer, whose permalloy screening cover was situated in a magnetically compensated environment in such a way as to make the residual magnetic field smaller than 1 nT at the point of measurement. Measurements of this type were made possible by the sensors of the ROCOMA magnetometer (Krs and Chvojka, 1987).

Palaeovolcanics

Below, we give examples of thermal demagnetization of Upper Cambrian andesites from the locality Trovice, Barrandian, the Bohemian Massif, and then of the Carboniferous tuff and Triassic andesites from Mongolia, region Tel Tin Gol.

In their natural state, Upper Cambrian andesites from the Barrandian are normally and reversely polarized. In the course of thermal demagnetization, the normally polarized samples were cleaned of pronunced secondary magnetization, and reverse directions were determined (see Fig. 7). Figures 8 and 9 present normalized graphs of remanent magnetization in dependence on the temperature, where M_t is the modulus of the remanent magnetic moment of the sample subjected to thermal demagnetization at a temperature of t (°C), M_0 being the modulus of the remanent magnetic moment of the sample in natural state. Below the normalized graphs of M_t/M_0, dependences of $æ_t/æ_0 = f(t)$ are given, where $æ_t$ is the apparent volume magnetic susceptibility of the sample subjected to thermal demagnetization at temperature t (°C) and $æ_0$ is the susceptibility of the sample in the natural state. Below are Zijderveld's diagrams (Zijderveld, 1967), in which full circles denote projections onto the horizon-

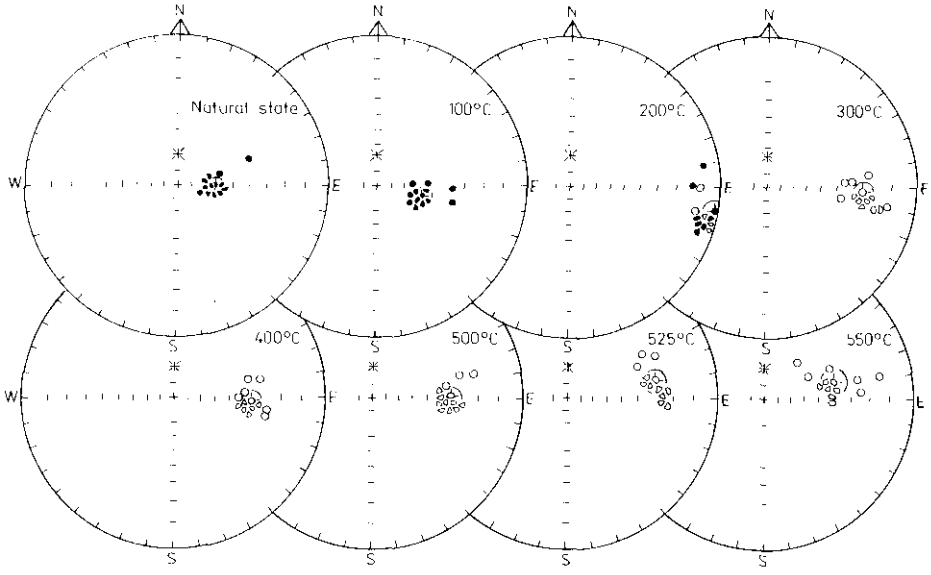

Fig. 7. Stereographic projection of directions of remanent magnetization of samples of Upper Cambrian andesite during thermal treatment, locality Týřovice, Barrandian, Bohemian Massif. Full (open) small circles indicate projection onto the lower (upper) hemisphere; a cross superimposed on a full (open) small circle indicates the mean direction; the trace of conficence cone (for P = 0.05) is denoted by a circle. Fisher's (1953) statistics were applied.

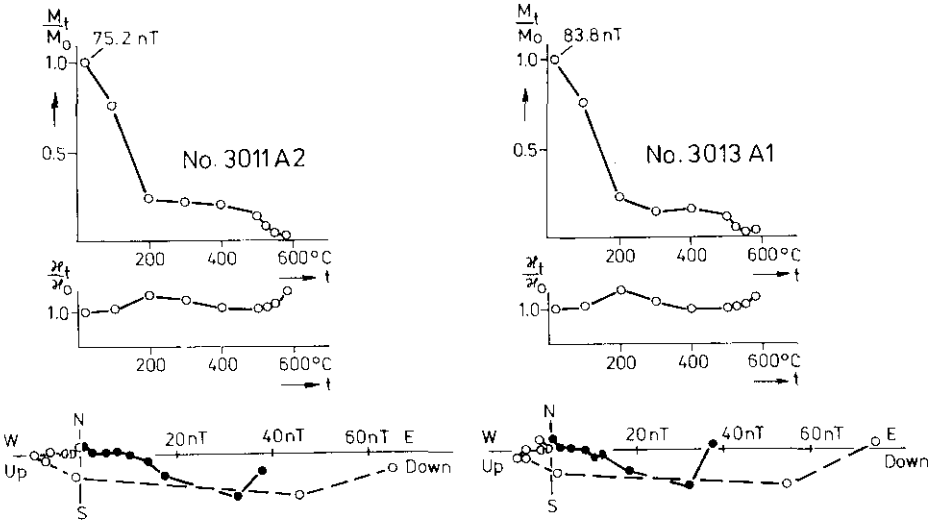

Fig. 8. Thermal demagnetization of samples of Upper Cambrian andesite. Locality Týřovice, Barrandian, Bohemian Massif.

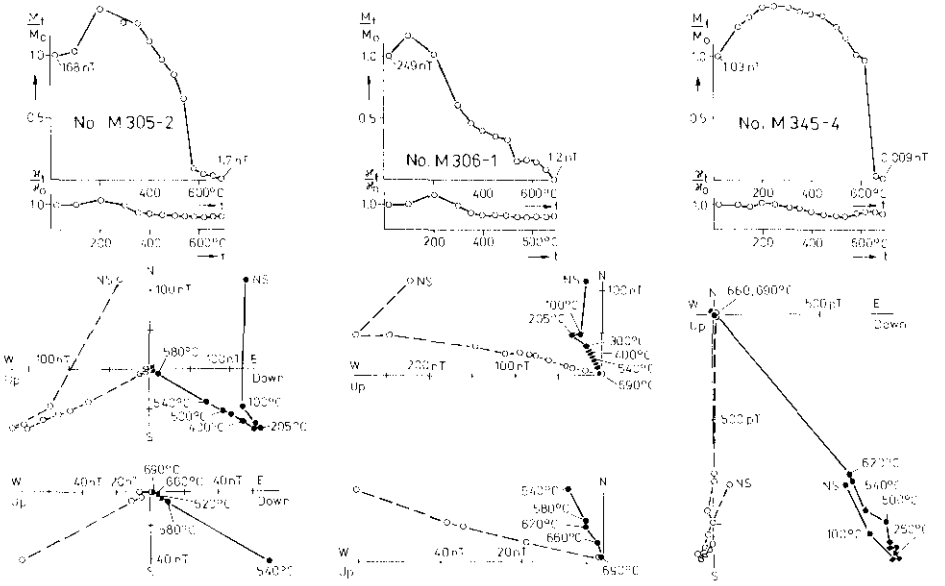

Fig. 9. Thermal demagnetization of two Triassic samples (Nos. M 305-2 and M 306-1) and a Carboniferous tuff (No. M 345-4) from the region of Tel Tin Gol, Mongolia. Data of P. Pruner.

tal plane and open circles denote projections onto the vertical N-S plane. The graphs of representative samples of Nos. 3011A2 and 3013A1 display a large proportion of secondary magnetization (Fig. 8). Reversely polarized samples in natural state, on the other hand, have mostly one-component magnetization.

The palaeomagnetic data derived from Mongolian rocks of three areas (Barun Buren, Tel Tin Gol, Chulut Tsagan Del) indicated a palaeogeographical affinity between the territories of north and south Mongolia and north China in the periods of the Triassic, Permian and the Carboniferous (Pruner, 1987). In the subsequent stage of investigations, sample collecting was greatly extended and the palaeomagnetic research confirmed the conclusions made in the preceding stage. The application of the MAVACS furnished good-quality laboratory data, examples of thermal demagnetization are given for three representative samples in Fig. 9. The graphs show individual magnetization components, the purity of thermal demagnetization is evident e.g. in samples of Nos. M 305-2 and M 306-1. In the lower part of the figures Zijderveld's diagrams are presented once more on an enlarged scale in the temperature interval 540 – 690 °C.

Sediments with detritic magnetization

The hitherto studied Middle Cambrian sediments of the Barrandian exhibited relatively low magnetization values, larger statistical sets therefore being used in data processing. Thermal demagnetization of Middle Cambrian greywacke from the locality Buchava — Slap, Barrandian, can be introduced as an example; the mean value of the remanent magnetization modulus is 184 pT ± 62 pT. Figure 10 shows the directions of thermally demagnetized samples, optimum cleaning was achievet at the temperature of 300 °C: D = 64.8°: α_{95} = 2,57°: k = 66.65 as the mean values of 47 samples.

Rocks of the same type were sampled in other localities and subjected to multi-component analysis. We present the results of progressive thermal demagnetization of weakly magnetic samples of the Middle Cambrian greywacke from another exposure in the locality Buchava — Slap, Barrandian. The mean directions of components A, B, C, D were computed with the use of Fisher's statistics (1953). Table 1 gives the directions of the respective components. Four magnetization components were identified; component A probably corresponds to the laboratory field, component B to the recent geomagnetic field, component C is statistically ill-defined and is apparantly of Variscan origin, component D is pre-Variscan. These results were collated and compared with data from other localities that were derived by the same procedures, see the work by Krs *et al.* (1987).

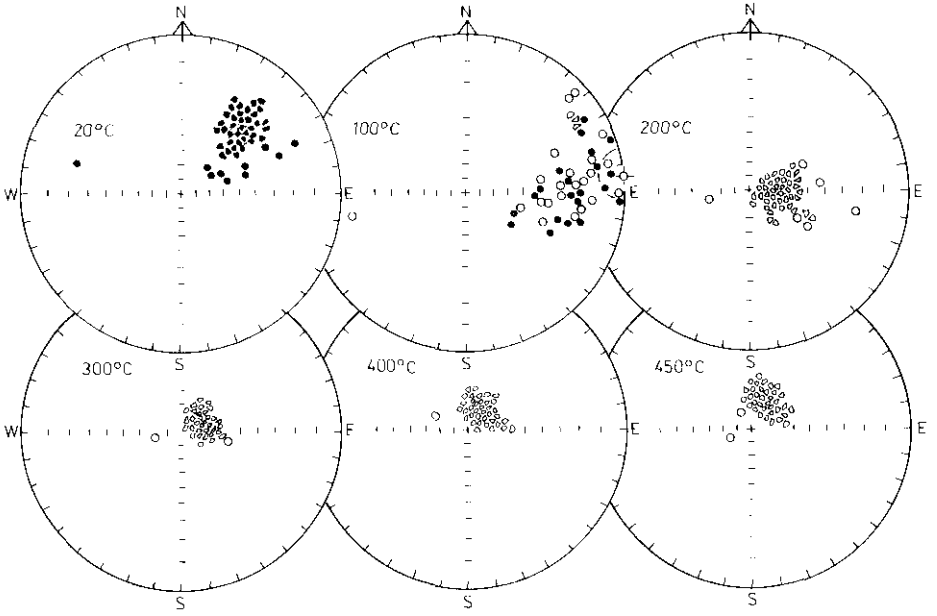

Fig. 10. Directions of remanent magnetization of samples of Middle Cambrian greywacke. Locality Buchava — Slap. Barrandian, Bohemian Massif.

Sediments with chemoremanent magnetization

For the purposes of palaeomagnetic research into the Ordovician rocks of the Barrandian, Bohemian Massif, samples of different geneses were collected, such as porphyrites, diabase rocks, tuffs and tuffites, oolitic haematite ores, haematite pigmented shales, greywackes and red silicites predominantly of the Lower Ordovician age (see Krs *et al.*, 1986). The samples were collected from the outcrops of both subhorizontally-lying and folded rocks to create conditions for combining laboratory tests of stability and of magnetic cleaning with fold tests. Interesting results were obtained in red silicites, in which, according to the petrographic analysis, the magnetization carrier was the haematite pigment: haematite as the principal carrier of undoubtedly chemoremanent magnetization was proved during thermal demagnetization. The samples of red silicites constitute a macroscopically as well as microscopically extraordinarily homogeneous rock with very fine dispersed haematite pigment. As far as the magnetic aspect is concerned, however, they are distinctly unhomogeneous and contain magnetization components of minerals ranging magnetically from extraordinarily soft to extraordinarily hard. In the samples with predominantly one-component magnetization, pre-Variscan palaeo-

TABLE 1

Mean directions of respective components of remanent magnetization of samples of Middle Cambrian greywacke, Nos. 3093A-3113A. Locality Buchava-Slap, Barrandian, Bohemian Massif.

Component of remanent magnetization	Temperature interval	Mean direction of remanent magnetization		α_{95}	k	n	Correction for dip of rocks
		Declination	Inclination				
A	20°-100° C	30.1°	42.8°	4.1°	53.8	24	YES
		14.3°	31.9°	3.8°	60.2	24	NO
B	Prevailingly 100°-300° C	111.3°	74.3°	6.3°	26.2	21	YES
		0.1°	79.2°	6.2°	27.2	21	NO
C	Prevailingly 300°-460° C	166.7°	−6.7°	49.0°	2.5	7	YES
		167.2°	11.9°	48.9°	2.5	7	NO
D	Prevailingly >460° C	0.4°	−79.7°	2.6°	171.2	18	YES
		109.1°	−74.6°	2.7°	164.6	18	NO

magnetic directions were established. The mean palaeomagnetic declination of these rocks amounts to 126.7 °, inclination to −41.7 °, $\alpha_{95} = 3.63$ °. The palaeogeographic latitudes computed from the palaeomagnetic data of the Lower Ordovician silicites follow up well with the results of the data of the Middle and Upper Cambrian of the Barrandian.

Strongly remagnetized rocks of the red beds type

In order to extend the magnetostratigraphic studies to the entire profile of the Permo-Carboniferous rocks of the Bohemian Massif, we also carried out methodical work with strongly remagnetized Lower Permian **red beds** from the Krknoše-piedmont and Intra-Sudetic Basins in the Bohemian Massif. Different variants of the multi-component analysis of remanent magnetization were applied including the modified method of great circles (Hall, 1978). The palaeomagnetic directions were obtained by means of two algorithms LINEFIND and Fisher's distribution, and second, with the use of the poles of remagnetization planes treated by Watson's distribution (by Chvojka in Krs *et. al.*, in press).

Figure 11 presents an example of Zijderveld's diagram for a strongly remagnetized sample, the circles around the full and open circles denote the scatter of repeated measurements on spinner magnetometer JR-4, the lower part of the figure contains enlarged Zijderveld's diagram for the temperature interval 620 — 685° C. Component A is conditioned by the effect of the recent geomagnetic field, component B of a very low value corresponds to the Lower Permian palaeomagnetic directions in the area of sample collection. Analogous results were obtained in other groups of samples. Component B was derived from the temperature interval 620 — 685° C, and although it only represents some percentage of natural remanent magnetization, the mean palaeomagnetic direction could be derived with sufficient accuracy.

Organogenic limestones

Palaeomagnetic research into the pre-Variscan formations of the Bohemian Massif also comprises investigations of the palaeomagnetic characteristics of the Devonian organogenic limestones in the Barrandian. These whitish to greyish limestones, with a certain share of clayey component, occur in the Devonian base. In the stratotype locality of Klonk, SW of Prague, there is an extensive exposure with a continuous sequence of limestone layers distinctly separated from one another from the Upper-most Silurian to the Lower Devonian, without a hiatus and lithologi-

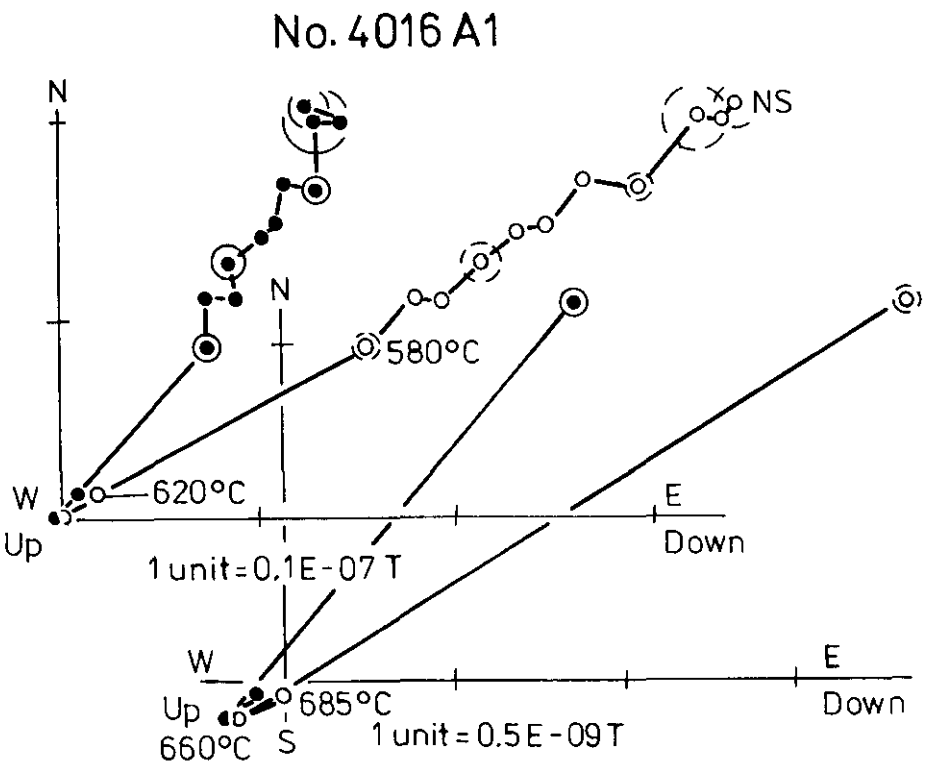

Fig. 11. Zijderveld's diagrams for a strongly remagnetized sample of Lower Permian rocks of the **red beds** type. Locality Hynčice. Bohemian Massif.

cal changes. Individual layers were marked in the field by numbers and this makes the locality convenient for further comparison studies.

Representative samples were subjected to combined demagnetization with the use of alternating and thermal fields, which was more effective than thermal demagnetization only. At first, the samples were demagnetized by aternating fields to relatively low fields of 12 m̃T as they were magnetically soft and in higher fields prone to the origin of anhysteretic magnetization. Following the alternating field demagnetization, the samples were subjected to progressive thermal demagnetization with the use of the MAVACS.

Fig. 12 gives as an example Zijderveld's diagrams for the samples subjected to combined demagnetization. Even though it involves samples with small values of remanent magnetization moduli and the samples are relatively magnetically soft, components A and B respectively are well defined. The results of the multi-component analysis by the LINEFIND method are presented in the next figure for the group of samples investigated. Components A and B directions are given in Fig. 13. The mean di-

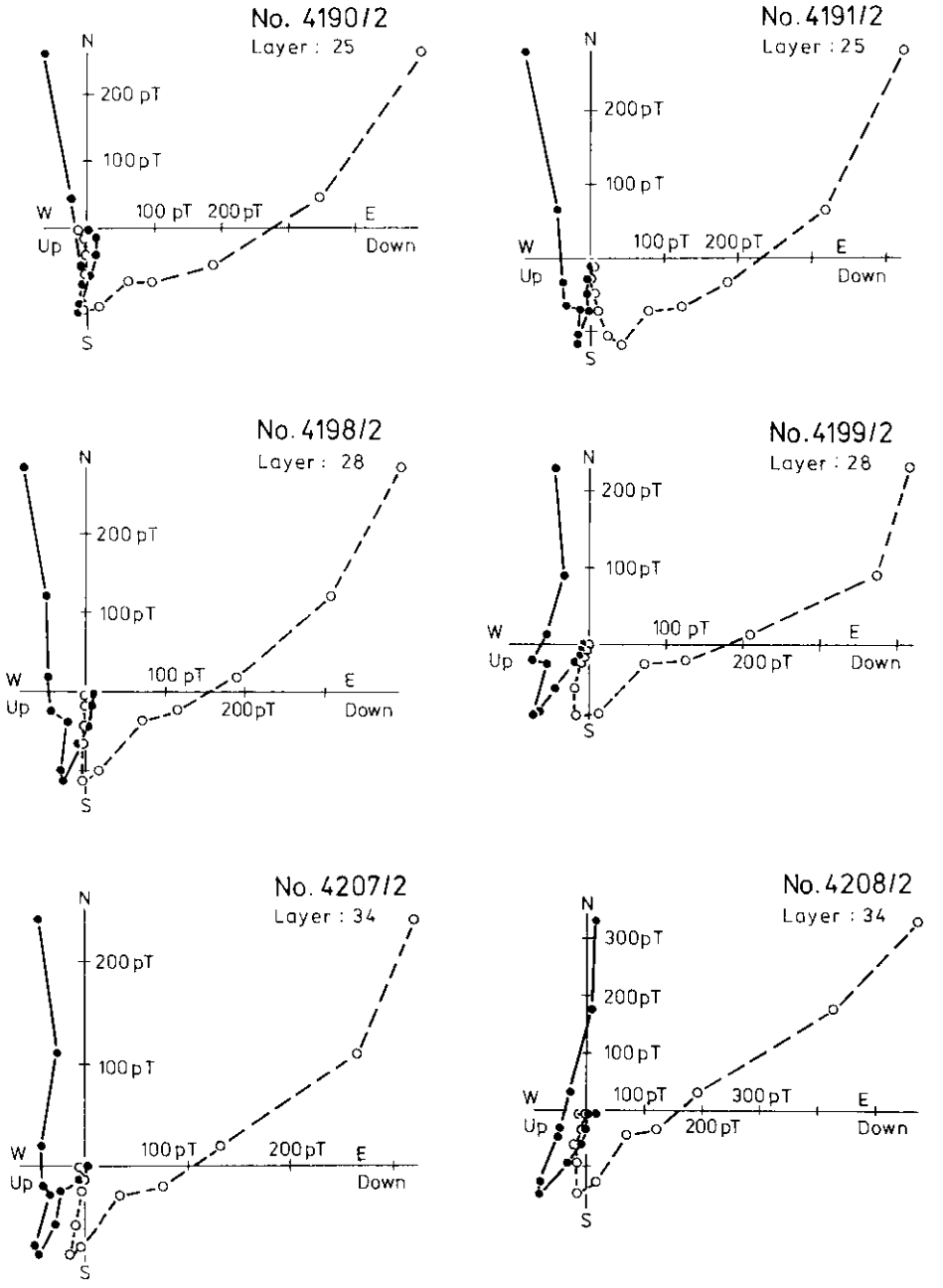

Fig. 12. Zijderveld's diagrams for samples of Lower Devonian limestone. Locality at the stratotype Klonk, Barrandian, Bohemian Massif.

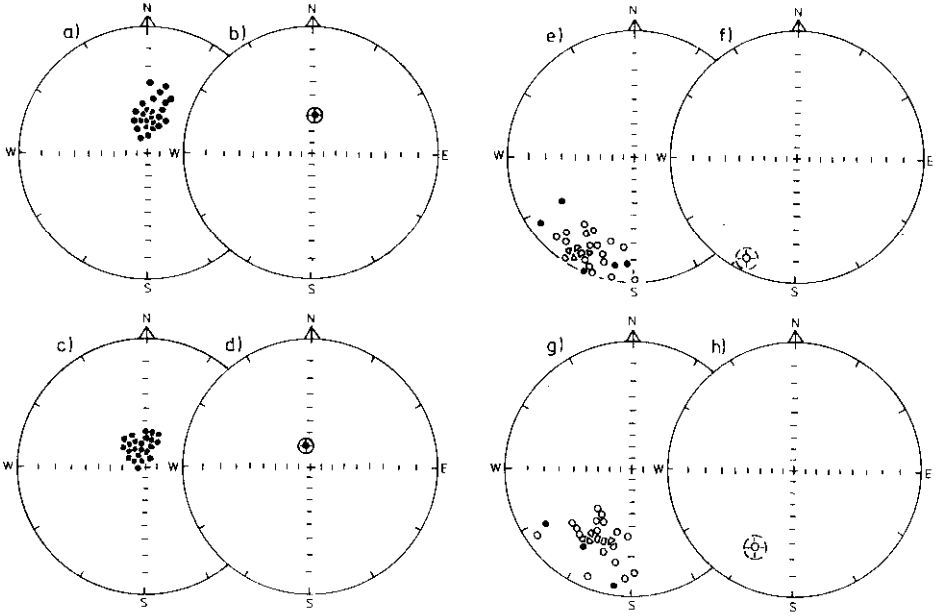

Fig. 13. Directions of components A and B of samples of Lower Devonian limestone, locality Klonk, Barrandian. a) Components A corrected for dip of strata. b) Mean direction for components A corrected for dip of strata. c) Components A not corrected for dip of strata. d) Mean direction for components A not corrected for dip of strata. e) Components B corrected for dip of strata. f) Mean direction for components B corrected for dip of strata. g) Components B not corrected for dip of strata. h) Mean direction for components B not corrected for dip of strata.

rection of component A agrees with the direction of the recent geomagnetic field. For the Bohemian Massif, the computed palaeomagnetic (virtual) pole position of component B falls within the Upper Carboniferous to Lower Permian pole positions, cf. Krs (1968). Thus, in the rocks under study, the original Lower Devonian palaeomagnetic directions were not preserved. Similar conclusion was earlier reached by Chamalaun and Creer (1963) and later by many others, the cited authors attributed a world-wide character to this phenomenon. In our case, the limestones are weakly magnetic, the carriers of magnetization being mainly hydro-oxides of Fe. Rock samples of similar magnetic properties can only be demagnetized if the magnetic field is perfectly compensated, otherwise undesirable partial thermo-remanent magnetic components would be generated in the samples in the course of laboratory thermal treatment.

CONCLUSION

The main objective was to develop and test a laboratory apparatus for palaeomagnetic and rock-magnetic research for securing the high magnetic vacuum needed during the demagnetization of rock samples. Rocks, affected by orogenic phases in general, display a number of magnetization components. Under thermal demagnetization in particular, in the course of which ferrimagnetic minerals with magnetically soft properties are created, precise laboratory procedures are required. In many cases it was necessary to carry out the multi-component analysis of magnetization on whole sets of rock samples, which, of course, imposed higher technical demands on the type of thermal demagnetizer. The innovative apparatus called MAVACS provides a magnetic vacuum with an accuracy higher than ± 2 nT in roughly 5 litres in volume, facilitating demagnetization of larger sets of samples.

The basic component of the MAVACS is the ROCOMA magnetometer, which indicates a true magnetic vacuum with a typical deviation of max. ± 0.1 nT. This feature, unique among magnetometers, was achieved by means of a special sensor utilizing a rotating coil (being borne and high-speed driven by compressed air), which also yields bidirectional sensor sensitivity and the non-magnetic quality fundamental for this application. MAVACS is thus free of magnetic parts and disturbing physical fields, which facilitates the further extension of its applications to magnetic metrology, geomagnetism and possibly SQUID magnetometry applied to biomagnetism.

REFERENCES

CHAMALAUN, F. H. and CREER, K. M., 1963. A revised Devonian pole for Britain. Nature, 198, No. 4878, 375.

CHVOJKA, R., 1987. Programmes for evaluation of palaeomagnetic and petromagnetic data — part I. Internal Report in Czech. Geofyzika N.C., Prague.

FISHER, R., 1953. Dispersion on a sphere. Proc. Roy. Soc., A, 217: 295-305.

HALL, H. C., 1978. The use of converging remagnetization circles in palaeomagnetism. Phys. Earth. Planet. Inter., 16: 1-11.

JELÍNEK, V., 1973. A high sensitivity spinner magnetometer. Stud. Geophys. Geod., 10: 58-78.

JELÍNEK, V., 1973. Precision A.C. bridge set for measuring magnetic susceptibility and its anisotropy. Stud. Geophys. Geod., 17: 36-48.

KENT, J. T., BRIDEN, J. C. and MARDIA, K. V., 1983. Linear and planar structure in ordered multivariate data as applied to progressive demagnetization of palaeomagnetic remanence. Geophys. J. Roy. astro. Soc., 75: 593-621.

KIRSCHVINK, J. L., 1980. The least squares line and plane and the analysis of palaeomagnetic data. Geophys. J. Roy. astro. Soc., 62: 699-718.

KRS. M., 1968. Rheological aspects of palaeomagnetism? XIII Internat. Geol. Congress, Prague, 5: 87-96.

KRS. M. and CHVOJKA, R., 1987. On the techniques of analysing the multi-component magnetization of rocks using the ROCOMA magnetometer. Stud. Geophys. Geod., 31: 176-196.

KRS. M., CHVOJKA, R. and VALÍN, F., in press. A contribution to methodology of magnetostratigraphic studies of strongly remagnetized Lower-Permian rocks, Bohemian Massif. Zeitschrift für geologische Wissenschaften.

KRS. M., KRSOVÁ, M., PRUNER, P., CHVOJKA, R. and HAVLÍČEK, V., 1987. Palaeomagnetism, palaeogeography and the multicomponent analysis of Middle and Upper Cambrian rocks of the Barrandian in the Bohemian Massif. In: D. V. Kent and M. Krs (Editors), Laurasian Paleomagnetism and Tectonics. Tecnophysics, 139: 1-20.

KRS, M., KRSOVÁ, M., PRUNER, P. and HAVLÍČEK, V., 1986. Paleomagnetism, paleogeography and multi-component analysis of magnetization Ordovician rocks from the Barrandian area of the Bohemian Massif. Sb. geol. Věd, Užitá Geofyz., 20: 9-45.

PEŠINA, B., 1986. A multi-purpose astatic magnetometer. Travaux Inst. Géophys. Acad. Tchécosl. Sci., Geofys. sbor. 1967, Academia, Prague, 278: 355-365.

PRUNER, P., 1987. Palaeomagnetism and palaeogeography of Mongolia in the Cretaceous, Permian and Carboniferous — preliminary data. In: D. V. Kent and M. Krs (Editors), Laurasian Paleomagnetism and Tectonics. Tectonophysics, 139: 155-167.

SCHMIDT, P. W., 1982. Linearity spectrum analysis of multi-component magnetizations and its application to some igneous rocks from south-eastern Australia, Geophys. J. Roy. astro. Soc., 70: 647-665.

ŠANDA, J., 1987. Instruction manual for KINT-2, Internal Report. in Czech. Geofyzika N. C., Prague.

ZIJDERVELD, J. D. A., 1967. A.C. demagnetization of rocks: Analysis of results. In: D. W. Collinson, K. M. Creer and S. K. Runcorn (Editros). Methods in Palaeomagnetism. Developments in Solid Earth Geophysics, 3: 254-295.

Received 7 Jan. 1988.
Accepted 13 June 1988.